ISSN 1674-1056
http://cpb.iphy.ac.cn
http://iopscience.iop.org/cpb
中国物理 B
Chinese Physics
中国物理 Chinese Physics B

Quantum intelligence on protein folding pathways

Wen-Wen Mao(毛雯雯)[1], Li-Hua Lv(吕丽花)[1], Yong-Yun Ji(季永运)[2], You-Quan Li(李有泉)[1,3]

Citation: Chin. Phys. B . 2020, 29(1): 018702 . **doi:** 10.1088/1674-1056/ab5fbe
Journal homepage: http://cpb.iphy.ac.cn; http://iopscience.iop.org/cpb

What follows is a list of articles you may be interested in

Quantum search for unknown number of target items by hybridizing fixed-point method with trail-and-error method

Tan Li(李坦), Shuo Zhang(张硕), Xiang-Qun Fu(付向群), Xiang Wang(汪翔), Yang Wang(汪洋), Jie Lin(林杰), Wan-Su Bao(鲍皖苏)

Chin. Phys. B . 2019, 28(12): 120301 . **doi:** 10.1088/1674-1056/ab4e88

On the usefulness of an assisted driving Hamiltonian for quantum adiabatic evolution

Jie Sun(孙杰), Songfeng Lu(路松峰)

Chin. Phys. B . 2018, 27(11): 110306 . **doi:** 10.1088/1674-1056/27/11/110306

Demonstration of quantum anti-Zeno effect with a single trapped ion

Man-Chao Zhang(张满超), Wei Wu(吴伟), Lin-Ze He(何林泽), Yi Xie(谢艺), Chun-Wang Wu(吴春旺), Quan Li(黎全), Ping-Xing Chen(陈平形)

Chin. Phys. B . 2018, 27(9): 090305 . **doi:** 10.1088/1674-1056/27/9/090305

Demonstration of quantum permutation parity determine algorithm in a superconducting qutrit

Kunzhe Dai(戴坤哲), Peng Zhao(赵鹏), Mengmeng Li(李蒙蒙), Xinsheng Tan(谭新生), Haifeng Yu(于海峰), Yang Yu(于扬)

Chin. Phys. B . 2018, 27(6): 060305 . **doi:** 10.1088/1674-1056/27/6/060305

Proteins：From sequence to structure

Zheng Wei-Mou

Chin. Phys. B . 2014, 23(7): 078705 . **doi:** 10.1088/1674-1056/23/7/078705

RAPID COMMUNICATION

Quantum intelligence on protein folding pathways*

Wen-Wen Mao(毛雯雯)[1], Li-Hua Lv(吕丽花)[1], Yong-Yun Ji(季永运)[2], and You-Quan Li(李有泉)[1,3,†]

[1] *Zhejiang Province Key Laboratory of Quantum Technology & Device and Department of Physics, Zhejiang University, Hangzhou* 310027, *China*

[2] *Department of Physics, Wenzhou University, Wenzhou* 325035, *China*

[3] *Collaberative Innovation Center of Advance Microstructure, Nanjing University, Nanjing* 210008, *China*

(Received 4 December 2019; accepted manuscript online 9 December 2019)

We study the protein folding problem on the base of our quantum approach by considering the model of protein chain with nine amino-acid residues. We introduce the concept of distance space and its projections on a XY-plane, and two characteristic quantities, one is called compactness of protein structure and another is called probability ratio involving shortest path. The concept of shortest path enables us to reduce the 388×388 density matrix to a 2×2 one from which the von Neumann entropy reflecting certain quantum coherence feature is naturally defined. We observe the time evolution of average distance and compactness solved from the classical random walk and quantum walk, we also compare the features of the time-dependence of Shannon entropy and von Neumann entropy. All the results not only reveal the fast quantum folding time but also unveil the existence of quantum intelligence hidden behind in choosing protein folding pathways.

Keywords: protein folding, quantum walk, shortest pathways, mean first passage time

PACS: 87.15.hm, 03.67.Ac, 05.40.Fb **DOI:** 10.1088/1674-1056/ab5fbe

1. Introduction

Protein folding problem has been an important topic in interdisciplinary field involving molecular biology, computer science, polymer physics as well as theoretical physics, *etc*. Levinthal noted early in 1967 that a much larger folding time is inevitable if proteins are folded by sequentially sampling of all possible conformations. It was widely assumed that a random conformational search does not occur in the folding process, for which various hypotheses with the help of a series of meta-stable intermediate states have been often proposed. There have been substantial theoretical models which are useful for understanding the essentials of the complex self-assembly reaction of protein folding with different simplifying assumptions, such as Ising-like model,[1,2] foldon-dependent protein folding model,[3] diffusion–collision model,[4,5] and nucleation-condensation mechanism.[6,7] However till now, this often brings in certain difficulties in connecting analytical theory to experimental results because some hypotheses can not be easily put into a practical experimental measurement since they often rely on various hypotheses.[8–12] As the approach of computing simulations introduced less hypotheses in comparison to those theoretical models, the atomistic simulations[13–15] have been also used to investigate the protein folding along with nowadays' advances in computer science. All-atom computational method,[16] including physics-based and knowledge-based approaches, have provided useful insights on protein folding and design by building high-accuracy atomistic models of proteins. However, all those models are computationally costly for high-throughput folding studies and still need certain artificial hypotheses.

Recently, we proposed a quantum strategy[17] without making hypotheses to formulate protein folding as a quantum walk on a definite graph, in which we merely studied the model with six amino-acids as toy model. We know the shortest peptide chain in nature contains more than twenty amino-acid residues. Toward a genuine understanding, it is obligatory to study more complicate case with more residues. Here we consider the model with nine amino-acid residues and obtain that the folding time via our quantum approach is much shorter than the one obtained via classical random walk. Moreover, as the number of amino acid residues increases, the set of protein structures and the corresponding connection graph become more complicate, which drives us to introduce the projection method and several characteristic quantities. After calculating and analyzing those quantities, we find some new features on the folding pathways in addition to the fast protein-folding time. Our quantum approach that employs and combines the concepts of quantum walk and mean first-passage time not only reveals fast protein-folding time but also unveils the existence of quantum intelligence on the protein folding pathways, which is expected to open a significant new area of research.

2. Model description

In the course-grained model the protein is considered as a chain of non-own intersecting unit[18–21] (usually referring an

*Project supported by the National Key Research and Development Program of China (Grant No. 2017YFA0304304) and the National Natural Science Foundation of China (Grant No. 11935012).

†Corresponding author. E-mail: yqli@zju.edu.cn

© 2020 Chinese Physical Society and IOP Publishing Ltd

amino acid residue) of a given length on the two-dimensional square lattice. We indicated recently[17] that for a protein with n amino-acid residues, there will be totally N_n distinct lattice conformations that distinguish various protein intermediate structures, which provide us a point set with N_n objects. We call such a point set as structure set and denote it by $\mathscr{S}_n = \{s_1, s_2, \ldots, s_{N_n}\}$. The entire structure set includes various structures that may be an unfolded, partially folded or completely folded. To distinguish their difference, we introduce a concept of compactness of a structure,

$$C = \frac{1}{n}\sum_{k=1}^{n}\left[|\boldsymbol{r}_k - \bar{\boldsymbol{r}}|^2\right]^{1/2}, \tag{1}$$

where the geometric center of the protein is located at $\bar{\boldsymbol{r}} = (\boldsymbol{r}_1 + \boldsymbol{r}_2 + \cdots + \boldsymbol{r}_n)/n$, and $\boldsymbol{r}_k$ refers to coordinates of the k-th residues. Clearly, the compactness $C_{\rm a}$ represents the average distance from each residues to its geometric center of a given structure $s_{\rm a}$. We consider in this paper the case of $n = 9$ and obtain $N_9 = 388$ through depth search algorithm (DSA). The 388 distinct structures that are unrelated by rotational, reflection or reverse-labeling symmetries[20] were plotted (see supplementary material, Table S1). The straight-line structure is labeled lastly as s_{388} for convenience since it is the farthest end of the depth-first algorithm search. We plot it together with the three most compact structures s_{186}, s_{193}, and s_{236} in Fig. 1 as an illustration. For the structure set $\mathscr{S}_9$, the compactness of each structure is calculated (see supplementary material, Table S2). The largest value $C = 2.222$ refers to the completely unfolded straight-line structure s_{388}, while the smallest value $C = 1.073$ refers to the most compact structure s_{186}, s_{193}, and s_{236}.

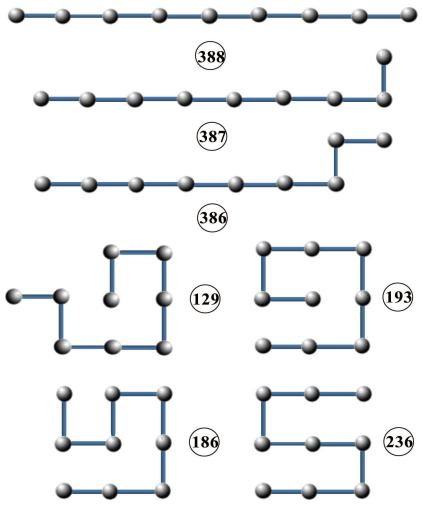


Fig. 1. Structure examples. There are 388 distinct structures for the amino-acid chain with 9 residues, thus the corresponding structure set $\mathscr{S}_9$ contains 388 objects. Here we plot the straight-line structure and the three most compact structures, together with three examples near to them via one or two one-step folding. For $n = 9$, the connection graph $\mathscr{G}_9$ includes 388 vertices which well defines the kinetic term of a quantum Hamiltonian.

In terms of the lattice model, we introduced previously the concept of one-step folding to describe the protein folding process.[17] The one-step folding is defined by one displacement of an amino acid in one of the lattice sites: two protein structures are connected via one-step folding if their chain conformations differ in one site only. For example, in Fig. 1, the structures s_{388} and s_{386} can be obtained by a one-step folding from s_{387}, and so did s_{193} from s_{129}. This enables us to establish certain connections between distinct objects in the structure set $\mathscr{S}_9$ so that we have a connection graph $\mathscr{G}_9$ which is described by a 388×388 adjacency matrix Mat(J_{ab}) that characterizes a classical random walk[22] on the connection graph.

3. Distance space and its projections

If the aforementioned graph $\mathscr{G}_n$ is completely connected, a distance between any two structures, saying s_a and s_b, is well defined. Then we will have a distance space $\mathscr{D}_n := \{s_a, d_{ab}\}$ in which the magnitude of d_{ab} equals the number of steps of the shortest path connecting s_a and s_b in the graph $\mathscr{G}_n$. There has been four line-crossings already when the 22-vertex graph $\mathscr{G}_6$ is plotted on a plane.[17] The $\mathscr{G}_9$ contains 388 vertices and appears very complicate if it is plotted on a plane. The largest distance in $\mathscr{D}_9$ stretches between the completely unfolded straight-line structure s_{388} and the most compact structures s_{186} or s_{193}, namely, $d_{388,186} = d_{388,193} = 17$. While the distance between the structure s_{388} and the other most compact structure s_{236} is no more the farthest, it is just $d_{388,236} = 14$.

It will be very helpful to make a projection of the space $\mathscr{D}_9$ into an XY-plane. If mapping the s_{388} to the origin point $(0,0)$ and either s_{186} or s_{193} to the farthest point at $(17,0)$, we will have a set of points in the XY-plane where each point corresponds to one or several objects in the space $\mathscr{D}_9$. Their concrete locations in the XY-plane are determined by the the distance away from $(0,0)$ and that away from $(17,0)$, respectively. The former represents the distance away from the straight-line structure s_{388} and the later represents that away from either s_{186} or s_{193} in the distance space $\mathscr{D}_9$.

The color scatter diagram shown in Fig. 2 exhibits the aforementioned projection of $\mathscr{D}_9$ on XY-plane, in which the color of each dot measures the degeneracy that is defined as the number of distinct structures mapping to the same point in the XY-plane. The degeneracy of each dot in the above figure and the concrete structures contained in the original images are all listed in supplementary material (see Table S3). Those points lain on the X axis in between $(0,0)$ and $(17,0)$ are the images of the objects referring to the shortest path leaving away from the initial structure s_{388} and approaching to a most compact structure. Those objects on the shortest path together with the one mapped to $(17,0)$ constitute a subset $S_{\rm I} \subset \mathscr{S}_9$. If let $S_{\rm II}$ denote the set constituted by the other objects, then the structure set $\mathscr{S}_9$ can be partitioned into two subsets $S_{\rm I}$ and $S_{\rm II}$, namely, $\mathscr{S}_9 = S_{\rm I} \oplus S_{\rm II}$.

The density matrix $\rho(t)$ describing quantum dynamics is of 388×388 that is too large to manifest some useful information. The above projection picture helps us to properly reduce the large density matrix to a 2×2 one to extract certain useful information, namely,

$$\tilde{\rho}=\begin{pmatrix}\rho_{\mathrm{I,I}} & \rho_{\mathrm{I,II}}\\ \rho_{\mathrm{II,I}} & \rho_{\mathrm{II,II}}\end{pmatrix}, \tag{2}$$

where $\rho_{\mathrm{I,I}}=\sum_a\rho_{aa}$, $\rho_{\mathrm{II,II}}=\sum_b\rho_{bb}$, $\rho_{\mathrm{I,II}}=\sum_{a,b}\rho_{ab}/\sqrt{N_{\mathrm{I}}N_{\mathrm{II}}}$ and $\rho_{\mathrm{II,I}}=\rho^*_{\mathrm{I,II}}$ with $a\in S_{\mathrm{I}}$, $b\in S_{\mathrm{II}}$ and N_{I}, N_{II} the total numbers of the objects in the corresponding subsets. Here the large density matrix stands for $\rho(t)=|\,\Psi(t)\rangle\langle\Psi(t)\,|$.

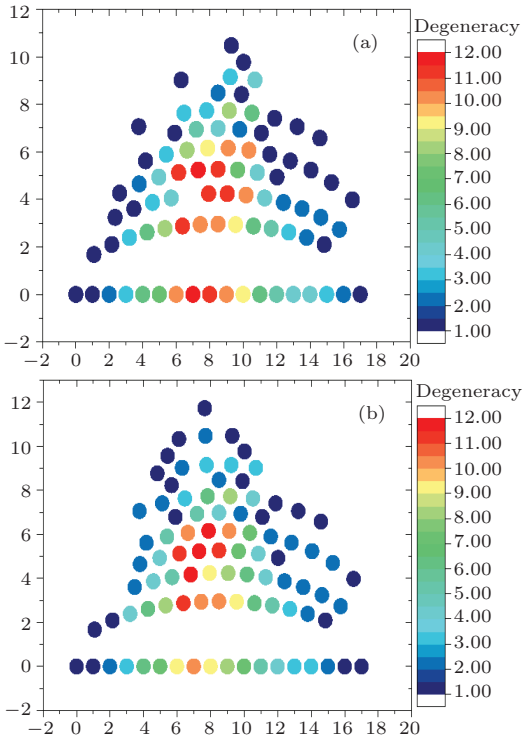


Fig. 2. Projection of the distance space $\mathscr{D}_9$. The color of the dot measures the degeneracy which is defined by the number of structures that concise on the same projection point. The points lain on X axis correspond to those structures on the shortest path. Here s_{388} was mapped to the origin point (0, 0), and (a) s_{186} as the farthest point, (b) s_{193} as the farthest point.

4. On the time evolution

Letting $|\,s_a\rangle$ denote the state of a protein structure in the shape of the a-th lattice conformation, we will have a quantum Hamiltonian in a 388-dimensional Hilbert space $\mathscr{H}=\{|\,s_a\rangle\,|\,a=1,2,\ldots,388\}$, namely, $\hat{H}=-\sum_{a,b}J_{ab}\,|\,s_a\rangle\langle s_b\,|$ where J_{ab} refers to the connections between different objects in the structure set $\mathscr{S}_9$, *i.e.*, J_{ab} is not zero if the a-th protein structure can be transited into the b-th one by a one-step folding while vanishes otherwise. With these physics picture one can investigate quantum walk[23–25] on the aforementioned graph, which gives a quantum mechanical understanding of the protein folding, *i.e.*, the process by which proteins achieve their native structure. As the time evolution is governed by the Schrödinger equation

$$\mathrm{i}\hbar\frac{\mathrm{d}}{\mathrm{d}t}|\,\Psi(t)\rangle=\hat{H}\,|\,\Psi(t)\rangle, \tag{3}$$

in which $|\,\Psi(t)\rangle=\sum_{a=1}^{388}\psi_a(t)\,|\,s_a\rangle$, and the expansion coefficients $\psi_a(t)$ can be solved numerically at least. In our numerical calculation, we set $\hbar$ and J to be unity and take the time step as $\Delta t=0.02$. For the initial condition, $|\,\Psi(0)\rangle=|\,s_{388}\rangle$, we solve the first-order differential equation (3) by means of Runge–Kutta method and obtain the magnitude of $\psi_a(t)$ at any later time, $t=j\cdot\Delta t$ with $j=1,2,\ldots$

In order to compare with the protein folding problem in the classical literature, *i.e.*, a random conformation search process, let us revisit the classical random walk. The continuous-time classical random walk[24] on a graph $\mathscr{G}_n$ is described by the time evolution of the probability distribution $p(t)$ that obeys the equation of motion

$$\frac{\mathrm{d}}{\mathrm{d}t}p_a(t)=\sum_b K_{ab}\,p_b(t), \tag{4}$$

where $K_{ab}=T_{ab}-\delta_{ab}$ with T_{ab} being the probability-transition matrix. In the conventional classical random walk, the probability-transition matrix is determined by the adjacency matrix of an undirected graph, namely, $T_{ab}=J_{ab}/\deg(b)$ where $\deg(b)=\sum_c J_{cb}$ represents the degree of vertex-b in the graph.

It is widely believed that the native structure of a protein possesses the lowest free energy.[26] This can be interpreted by the hydrophobic force that drives the protein to fold into a compact structure with as many hydrophobic residues inside as possible.[19] How fast does a protein initially in a straight-line structure fold into the most compact structure and what is the main behavior during the folding process will be important issues to study.

5. Folding time and folding pathway

We let $P_{a,b}(t)$ denote the probability of a state being the basis state $|\,b\rangle$ at time t if starting from the state $|\,a\rangle$ at initial time $t=0$. Quantum mechanically, $P_{a,b}(t)=|\psi_b^{(a)}(t)|^2$ as long as we solved the Schrödinger equation (3) in terms of the initial condition $|\,\Psi(0)\rangle=|\,s_a\rangle$. Here the superscripts are introduced to distinguish the solution from different initial conditions. As we know, the first-passage probability $F_{a,b}(t)$ from a state $|\,s_a\rangle$ to another state $|\,s_b\rangle$ after t time obeys the known convolution relation[27–31]

$$P_{a,b}(t)=\int_0^t F_{a,b}(t')P_{b,b}(t-t')\mathrm{d}t', \tag{5}$$

where $P_{b,b}(t)=|\psi_b^{(b)}(t)|^2$ arises from the solution of Eq. (3) from another initial condition $|\,\Psi(0)\rangle=|\,s_b\rangle$. In the classical

case, $P_{a,b}$ and $P_{b,b}$ refer to the $p_b(t)$ solved from Eq. (4), respectively, with initial conditions $p_c(0)=\delta_{ac}$ and $p_c(0)=\delta_{bc}$.

As protein folding is the process that proteins achieve their native structures, the folding time is the case that the starting state is chosen as $|s_{388}\rangle$ and the target states are the most compact states $|s_c\rangle$. For example, they are $|s_{186}\rangle$, $|s_{193}\rangle$ for $n=9$ as aforementioned. With the help of the first-passage probability solved from Eq. (5), we can calculate the folding time by the formula

$$\tau_{\rm fd}=\frac{\int_0^{\tau_0} tF_{a,c}(t)\mathrm{d}t}{\int_0^{\tau_0} F_{a,c}(t)\mathrm{d}t}, \tag{6}$$

where τ_0 represents the time period when the first-passage probability vanishes $F_{a,b}(\tau_0)=0$ firstly.[17] Here $a=388$ and $c=186$ or 193. We know in a previous work that the quantum folding is faster than the classical folding with about four to six times even for the simplest model of 4 residues and it is faster than the classical folding with almost ten to hundred times or more for $n=6$.[17] Here we calculate the folding time for $n=9$ that is given in Table 1. We can see that the quantum folding time $\tau_{\rm fd}^{\rm q}$ is much shorter than the classical folding time $\tau_{\rm fd}^{\rm c}$, and their difference becomes more significant in the case of $n=9$ in comparison to that of $n=6$.

Table 1. The probability ratio and the folding time.

Structure	$\bar{\gamma}^{\rm q}$	$\bar{\gamma}^{\rm c}$	$\tau_{\rm fd}^{\rm q}$	$\tau_{\rm fd}^{\rm c}$
s_{186}	0.341002	0.551697	8.549224	2153.938
s_{193}	0.353285	0.542997	6.440695	3305.09

In order to explore whether there are any intelligence hidden behind in choosing the protein-folding pathway, we compare the total probability on the shortest path and the other path by a probability ratio γ to demonstrate how it changes relatively after it leaves the initial state, namely,

$$\gamma(t)=\frac{\Gamma_{\rm II}(t)-P_{a,a}(t)}{\Gamma_{\rm I}(t)}, \tag{7}$$

where $\Gamma_\sigma(t)=\sum_{b\in S_\sigma}P_{a,b}(t)$ with $\sigma={\rm I},{\rm II}$. Our result is plotted in Fig. 3, we can see that the magnitude of γ changes from 0 to 1 monotonously during a short period of time for both quantum and classical cases. This implies that the probability on the shortest path is more favorable after leaving the initial state for it is on the denominator of γ. In order to rule out the ambiguity on the time scales about classical and quantum literature, we evaluate a mean ratio, $\bar{\gamma}=\int_0^{\gamma=1}\gamma(t)\mathrm{d}t/\int_0^{\gamma=1}\mathrm{d}t$ and show them in Table 1. The mean ratio in quantum case $\bar{\gamma}^{\rm q}$ is smaller than that in classical case $\bar{\gamma}^{\rm c}$. This implies that the probability distribution is more aggregated on the shortest path in quantum case.

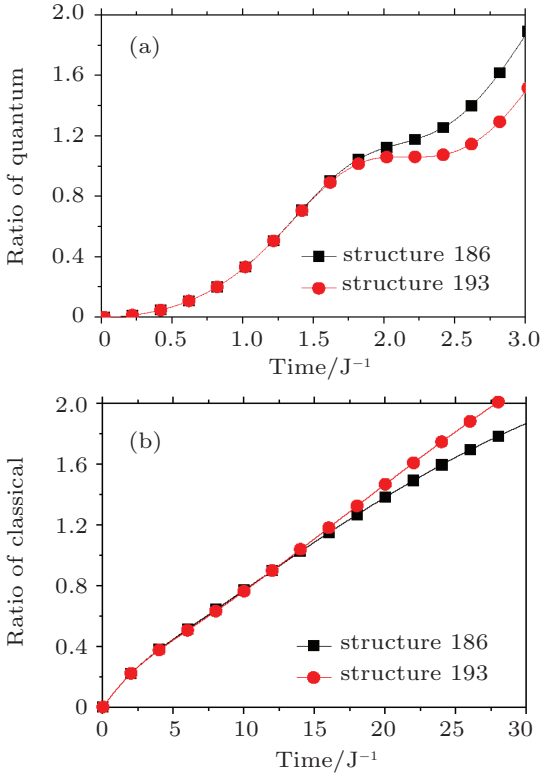


Fig. 3. The probability ratio γ. The time evolution of the folding process from s_{388} to s_{186} and s_{193} for (a) quantum walk and (b) classical random walk.

6. More on folding behavior

Although the random walk reflects a stochastic process, it is characterized by the probability distribution defined on all the distinct structures that can always give us intuitive information if we calculate some weighted average of the entire system. We can attain the time dependence of mean distance away from any structure s_a by calculating $\sum_b d_{ab}|\psi_b^{(a)}(t)|^2$. We can also observe the time evolution of the mean compactness $\sum_b C_a|\psi_b^{(a)}(t)|^2$. In classical case, the mean distance and mean compactness is evaluated by $\sum_b d_{ab}p_b^{(a)}(t)$ and $\sum_b C_a p_b^{(a)}(t)$ respectively. Our calculation of those two average quantities are given in Fig. 4. We can see that the mean distance of leaving away from the initial straight-line structure s_{388} increases much more rapidly in the quantum folding process than in classical case (see Fig. 4(a)). Correspondingly, the mean distance approaching to the most compact structures s_{186} and s_{193} decreases more rapidly (see Figs. 4(b) and 4(c)) in the quantum folding process than in classical one. Additionally, the average of compactness also decreases more rapidly in the quantum folding process than in class case (see Fig. 4(d)), thus the protein classically shrinks slower and it quantum mechanically shrinks faster.

As we know, quantum mechanically, the off-diagonal elements of a density matrix reflect certain quantum coherent properties, but our discussion till now have not yet involve it

directly. The partition of entire structure set into subset by considering the concept of shortest path helps us to have a 2×2 density matrix. It is then worthwhile to calculate von Neumann entropy[32] $E_{\rm N}(\tilde{\rho}) = -{\rm tr}(\tilde{\rho}\log_2\tilde{\rho})$. We also calculated the Shannon entropy[33] $E_{\rm S} = -p_{\rm I}\log_2 p_{\rm I} - p_{\rm II}\log_2 p_{\rm II}$ for the classical result to compare. Here $p_{\rm I} = \sum_{a\in S_{\rm I}} p_a$ and $p_{\rm II} = \sum_{b\in S_{\rm II}} p_b$. The aforementioned 2×2 density matrix $\tilde{\rho}$ can also define a quantity called the degree of coherence[34,35] $\eta(t) = 2{\rm tr}\tilde{\rho}(t)^2 - 1$, which is related to various quantum coherence phenomena, such as Rabi oscillation, self-trapping, *etc*. After making some calculus, one can find that the degree of coherence and the von Neumann entropy reach the extreme value at the same time, precisely, $\eta(t)$ takes minimal value when $E_{\rm N}(t)$ takes its maximum.

The time dependence of both von Neumann and Shannon entropies are plotted in Fig. 5. We can see that both entropies change from 0 monotonously to a maximal value and then varies. The maximal von Neumann entropy means the quantum state is in a completely mixed state (the degree of coherence vanishes), while a maximal Shannon entropy implies the maximal information uncertainty. In our present problem, the population (or probability summation in classical case) on the shortest path is dominated during the time before the entropy reaches the maximal value. Clearly, such a period in quantum case is longer than in classical case. This illustrates from another angle of view that quantum folding process posses more intelligence in protein folding pathway.

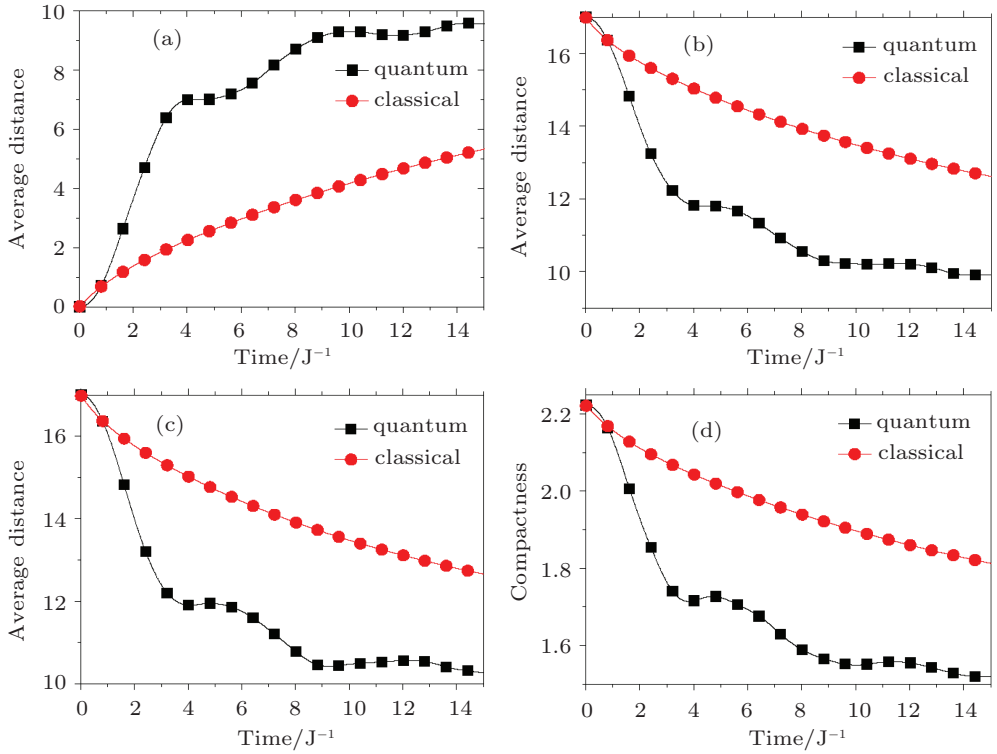


Fig. 4. The time evolutions of average distance and compactness. (a) The average distance leaving away from the initial structure s_{388}. (b) The average distance approaching to the most compact structure s_{186} while leaving from the structure s_{388}. (c) The average distance approaching to the most compact structure s_{193} while leaving from the structure s_{388}. (d) The time dependence of the overall average of compactness.

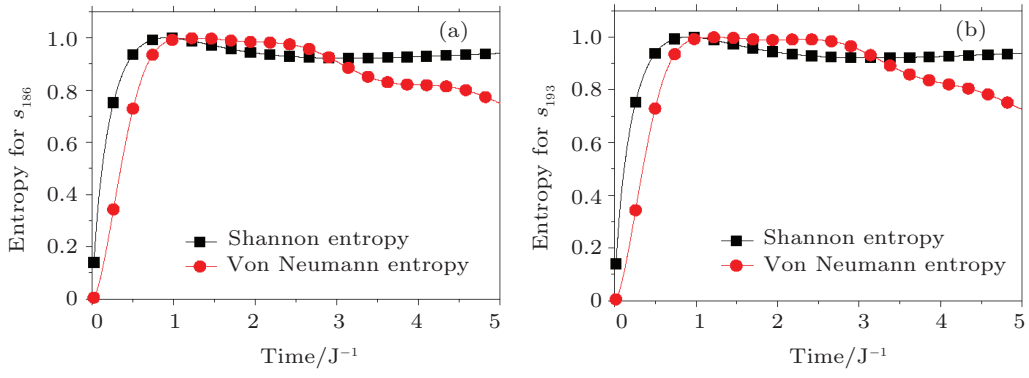


Fig. 5. The time-dependence of the entropy. (a) The quantum and classical time evolution of the entropy from s_{388} to s_{186}. (b) The quantum and classical time evolution of the entropy from s_{388} to s_{193}.

7. Summary

In the above, we studied the protein folding problem on the base of the quantum approach we proposed recently[17] by considering the model of protein chain with nine amino-acid residues. We have shown that the protein folding can be modelled as a quantum walk on the graph $\mathscr{S}_9$ of 388 vertices. As such a graph appears complicate if it were plotted on a plane, we introduced the concept of distance space $\mathscr{D}_9$ and its projections on a XY-plane by choosing two farthest structures (one is the completely unfolded straight-line structure and the other is a most compact structure) as reference-base points. According to our scheme,[17] we obtained the protein folding time by making use of the first-passage probability. In order to attain more understandings on the folding behavior, we introduced two characteristic quantities, one is called compactness of protein structure and the other is called probability ratio involving shortest path. The introduction of the concept of shortest path help us to reduce the 388×388 large density matrix to a 2×2 density matrix. Then we can conveniently evaluate the von Neumann entropy, *etc*. We also calculated the Shannon entropy on the base of classical random walk approach to compare. Our results not only confirmed the fast quantum folding time[17] but also unveiled that a quantum intelligence hidden behind in the choosing protein folding pathways.

References

[1] Mũnoz V and Eaton W A 1999 *Proc. Natl. Acad. Sci. USA* **96** 11311
[2] Henry E R and Eaton W A 2004 *Chem. Phys.* **307** 163
[3] Englander S W and Mayne L 2017 *Proc. Natl. Acad. Sci. USA* **114** 8253
[4] Karplus M and Weaver D L 1976 *Nature* **260** 404
[5] Sali A, Shakhnovich E and Karplus M 1994 *Nature* **369** 248
[6] Guo Z Y and Thirumalai D 1995 *Biopolymers* **36** 83
[7] Fersht A R 2000 *Proc. Natl. Acad. Sci.* **97** 1525
[8] Oliveberg M and Wolynes P G 2005 *Q. Rev. Biophys.* **38** 245
[9] Shakhnovich E 2006 *Chem. Rev.* **106** 1559
[10] Wolynes P G, Eaton W A and Fersht A R 2012 *Proc. Natl. Acad. Sci. USA* **109** 17770
[11] Dill K A and MacCallum J L 2012 *Science* **338** 1042
[12] Thirumalai D, Liu Z X, O'Brien E P and Reddy G 2013 *Curr. Opin. Struct. Biol.* **23** 22
[13] Piana S, Lindorff-Larsen K and Shaw D E 2012 *Proc. Natl. Acad. Sci. USA* **109** 17845
[14] Henry E R, Best R B and Eaton W A 2013 *Proc. Natl. Acad. Sci. USA* **110** 17880
[15] Snow C D, Nguyen H, Pande V and Gruebele M 2002 *Nature* **420** 102
[16] Mirny L and Shakhnovich E 2001 *Annual Review of Biophysics and Biomolecular Structure* **30** 361
[17] Lu L H and Li Y Q 2019 *Chin. Phys. Lett.* **36** 080305
[18] Taketomi H, Ueda Y and Go N 1975 *Int. J. Prept. Protein Res.* **7** 445
[19] Dill K A 1985 *Biochemistry* **24** 1501
[20] Li H, Helling R, Tang C and Wingreen N S 1996 *Science* **273** 666
[21] Li Y Q, Ji Y Y, Mao J W and Tang X W 2004 *Phys. Rev. E* **72** 021904
[22] van Kampen N G 1997 *Stochastic Processes in Physics and Chemistry* (revised edition) (Amsterdam: North-Holland)
[23] Aharonov Y, Davidovich L and Zagury N 1993 *Phys. Rev. A* **48** 1687
[24] Farhi E and Gutmann S 1998 *Phys. Rev. A* **58** 915
[25] Manouchehri K and Wang J B 2014 *Physical Implementation of Quantum Walks* (Berlin: Springer-Verlag)
[26] Anfinsen C B 1973 *Science* **181** 223
[27] Montroll E W 1969 *J. Math. Phys.* **10** 753
[28] Redner S 2001 *A guide to first-passage processes* (Cambridge: Cambridge University Press)
[29] Noh J D and Rieger H 2004 *Phys. Rev. Lett.* **92** 118701
[30] Condamin S, Benichou O, Tejedor V, Voituriez R and Klafter J 2007 *Nature* **450** 77
[31] Guerin T, Levernier N, Benichou O and Voituriez R 2016 *Nature* **534** 356
[32] Nielsen M A and Chuang I L 2000 *Quantum computation and quantum information* (Cambridge: Cambridge University Press)
[33] Pathria R K and Beale D P *Statistical Mechanics*, 3rd edn. (New York: Butterworth–Heinemann Elsevier)
[34] Leggett A J 2001 *Rev. Mod. Phys.* **73** 307
[35] Lu L H and Li Y Q 2009 *Phys. Rev. A* **80** 033619